Medical Engineering and Physics 69 (2019) 116–122

Contents lists available at ScienceDirect

Medical Engineering and Physics

journal homepage: www.elsevier.com/locate/medengphy

Developing and using fast shear wave elastography to quantify physiologically-relevant tendon forces

S.M. Hassan Ahmadzadeh[a,1,*], Xiao Chen[a,b,1], Henrik Hagemann[a], Meng-Xing Tang[a], Anthony M.J. Bull[a]

[a] Department of Bioengineering, Imperial College London, London SW72AZ, UK
[b] School of Electronic and Information Engineering, Nanjing University of Information Science and Technology, Nanjing, China

ARTICLE INFO

Article history:
Received 17 September 2018
Revised 7 April 2019
Accepted 14 April 2019

Keywords:
Shear wave elastography
Tendon forces
Shear wave speed
Tensile testing
Musculoskeletal models' validation

ABSTRACT

Direct quantification of physiologically-relevant tendon forces can be used in a wide range of clinical applications. However, tendon forces have usually been estimated either indirectly by computational models or invasively using force transducers, and direct non-invasive measurement of forces remains a big challenge. The aim of this study was to investigate the feasibility of using Shear Wave Elastography (SWE) for quantifying human tendon forces at physiological levels. An experimental protocol was developed to measure Shear Wave Speed (SWS) and tensile force in a human patellar tendon using SWE and conventional tensile testing to quantify the correlation between SWS and load. The SWE system was customised to allow imaging of fast shear waves expected in human tendons under physiological loading which is outside the normal range of the existing SWE systems. SWS increased from 10.8 m/s to 36.1 m/s with the increasing tensile load from 8 N to 935 N and a strong linear correlation between SWS and load ($r = 0.99$, $p < 0.01$) was observed. The findings in this study suggest that SWE can be used as a potential non-invasive method for direct quantification of physiologically-relevant tendon forces, as well as for validating the estimated forces from other methods such as computational models.

1. Introduction

Tendons attach muscle to bone and transmit tensile force due to muscular contraction to produce motion [1]. As such, tendons are subjected to considerable mechanical stresses and tensile forces during various activities and measurement of in-vivo tendon forces can provide a quantitative description of the tendon-muscle force transmission in production of movement which can be employed to evaluate the biomechanical properties of the musculoskeletal (MSK) system. Knowledge of tendon forces can be used in the diagnosis and treatment of MSK disorders such as tendon pathologies [2] and simulating tendon transfer surgery [3,4].

Tendon forces can be estimated indirectly by MSK models [5,6] or through measurements of strain, cross-sectional area (CSA) and stiffness of tendon using ultrasound elastography techniques [7–14]. Direct measures of tendon forces have been obtained using invasive force transducers [15,16]. Ultrasound elastography techniques have been typically used for measuring the stiffness of tendon as quantification of tendon forces using this technique requires accurate characterisation of viscoelastic properties of tendon. Therefore, considering the technical difficulties in validating MSK models and converting ultrasound strain measures to stress and load, as well as the invasiveness of using transducers, there is a need to develop non-invasive techniques to quantify tendon forces directly.

Shear Wave Elastography (SWE) is an emerging ultrasound-based imaging technique that quantifies mechanical properties of soft tissues by measuring Shear Wave Speed (SWS) propagation within the tissue [17–20]. This technique works based on a remotely-induced mechanical excitation and ultrafast imaging of the resulting shear wave propagation to calculate the SWS within the tissue. This technique has been widely implemented to characterise mechanical properties of various soft tissues including: liver [21], prostate [22], breast [23,24], brain [25], carotid artery [26] and MSK tissues [20].

Among MSK tissues, several studies have used SWE to quantify mechanical properties of muscles [27–32], ligaments [33] and tendons [19,34–41]. In these studies, SWS has been measured to characterise the length- and activation-dependence of stiffness changes in MSK tissues. The length-dependence of stiffness changes has been investigated by measuring the stiffness of

* Corresponding author.
E-mail address: mh.ahmadzadeh@gmail.com (S.M.H. Ahmadzadeh).
[1] These authors contributed equally to this work.

https://doi.org/10.1016/j.medengphy.2019.04.005
1350-4533/

the tissue under different conditions such as the resting position [29,36,37,41] or passive tension at various positions [19,34,35,38–40]. The activation-dependence of stiffness changes has been characterised by measuring the stiffness during static [28,30,31,42] or dynamic muscle contraction [27,28,42]. However, despite recent advances in the SWE technique, there are two major limitations in all of these studies that hinder the application of SWE for direct quantification of physiologically-relevant loadings in tendons.

Firstly, in these studies, tissue stiffness has been mostly characterised in terms of Young's modulus [35,36] or shear modulus [28–30,37,39,41] by using the assumption of an isotropic linear elastic tissue. However, tendons demonstrate non-linear, viscoelastic, transversely isotropic behaviour [18,43–45]. Therefore, some studies used SWS only to characterise the stiffness of MSK tissues [28,34,38,46]. Although these studies reported that SWS and stiffness increase by increasing the load, the direct relationship between tensile force, mechanical stress and SWS in human tendons remained unexplored.

Secondly, even though the results of the SWE studies have shown promise to characterise the stiffness of tendons at controlled postures, or to investigate the load-dependent changes of stiffness at low levels of muscle activation [27,34,42], the stiffness of tendon under physiological loading has not been adequately investigated.

Tendons of the lower limb are typically loaded up to one-quarter of their ultimate tensile stress during normal physiological activities [47]. This converts to a range from 6 MPa to 23 MPa for patellar tendon [48,49]. Others have estimated higher stresses up to 67 MPa during normal activities [50]. Although these estimates depend on the individual tendon, the intensity and type of physiological activity, it is evident that lower limb tendons are subjected to forces that are considerably higher than those investigated in previous SWE studies. The higher stiffness of tendons compared to muscles results in higher SWS that usually exceeds the range of SWS that can be detected by existing SWE systems. This issue has been conclusively reported as a key limitation of SWE with MSK

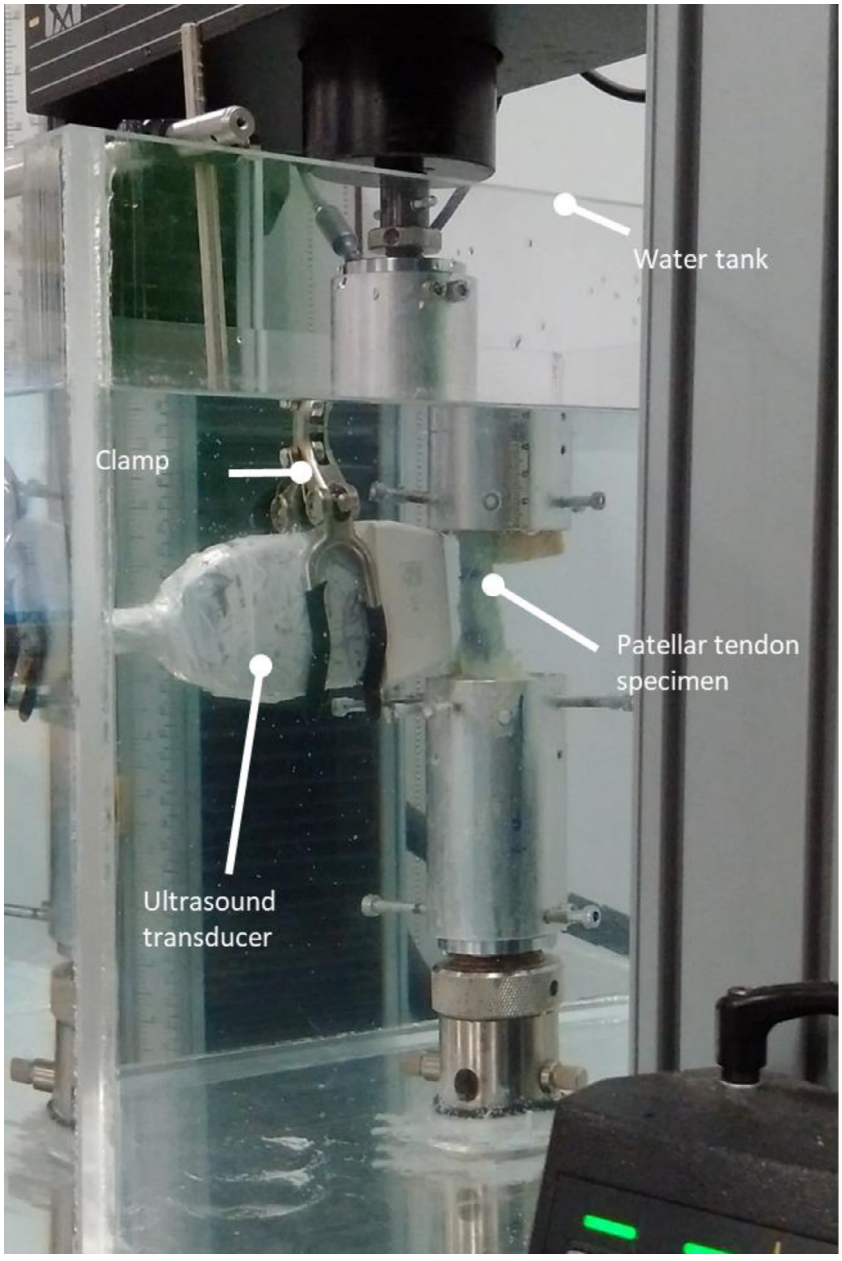

Fig. 1. The experimental setup for combination of SWE and tensile test.

tissues [27,28,30,34–42]. Therefore, a technical improvement is required to enable the measurement of higher SWS and therefore investigate mechanical properties of tendons with high stiffness under more physiologically-relevant loading. Thus, the aims of this study are to:

- find the direct correlation between tensile force, tensile stress and SWS in a cadaveric human patellar tendon using conventional tensile testing and SWE; and
- use an improved SWE system to estimate the SWS in tendon (with high stiffness) under high tensile loading and evaluate the feasibility of using the SWE technique as a direct measurement technique to estimate physiologically-relevant tendon forces for validating MSK models.

2. Materials and methods

2.1. Patellar tendon specimen preparation

A human cadaveric knee was harvested from the left leg of a male donor (age: 48 years). The patellar tendon with the entire patella and part of tibial bone, including the tibial tuberosity, was isolated by removing skin, muscles and knee ligaments. The tibial bone was cut into a block using a saw in order to fit in a custom-made pot for tensile testing. The tibial bone block and the patella were placed into the custom-made cylindrical aluminium pots and secured by alignment screws. The tendon was carefully aligned so that it was coaxial with the direction of loading of the materials testing machine. The patellar tendon was then set in polymethylmethacrylate bone cement before tensile testing. Ethical approval was granted from the Tissue Management Committee of the Imperial College Tissue Bank ethics committee (reference number: 12-WA-0196).

2.2. Cross-sectional area of the tendon

Tendon CSA was measured using a previously-validated protocol for soft tissues [51]. This protocol consisted of creating a cast of the tendon using stiff alginate paste (Blueprint cremix, Dentsply DeTrey, Germany), sectioning the cast along the length, taking photographs and using image analysis to calculate a mean CSA.

2.3. Tensile test

A tensile test was conducted using a screw-driven electromechanical materials testing machine (Instron 5866, 10 kN load cell with ± 0.5% accuracy, Canton, MA, USA). The tendon was mounted onto the materials testing machine so that the direction of the tendon fibres was parallel to the loading axis (Fig. 1). Load-elongation data were acquired at a sampling rate of 10 Hz using Bluehill software (v2.11, Instron, High Wycombe, UK).

2.4. Shear wave elastography measurements

2.4.1. Ultrasound imaging system

A Verasonics programmable ultrasound imaging system (Vantage, Verasonics Inc., Redmond, WA, USA) with a conventional linear transducer array (L7-4, 5 MHz, Philips healthcare, Bothell, WA, USA) was used to perform the SWE measurements. The system allows imaging a frame rate of up to 20,000 frames/s at an imaging depth of 3 cm. This system enables the focal depth of the push beam to be controlled so that strong shear waves can be generated at the region of interest (ROI).

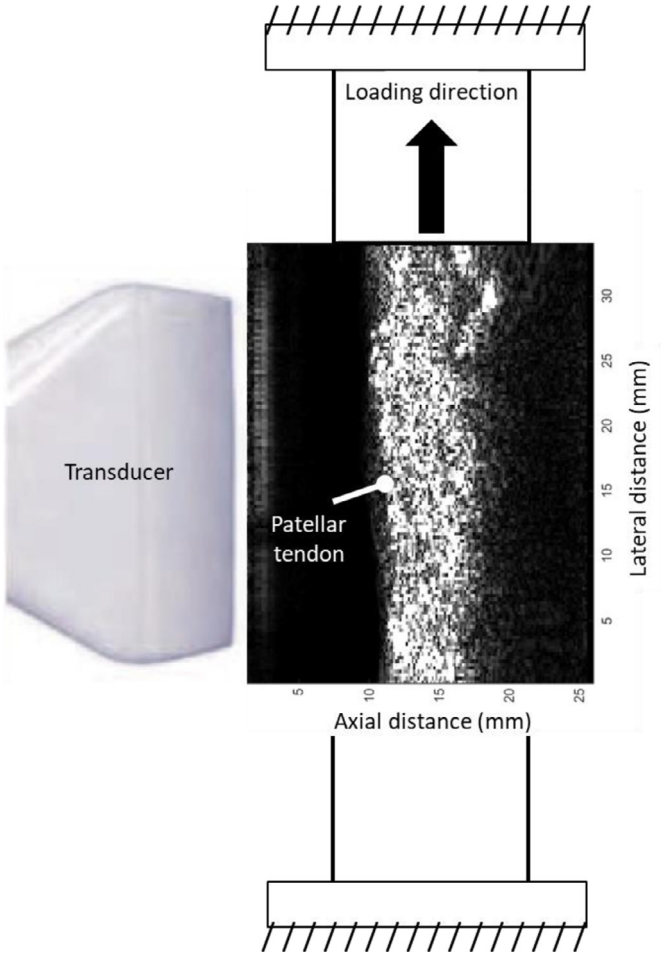

Fig. 2. A typical example of the B-mode image illustrating the position of the ultrasound transducer and the patellar tendon under tension. The B-mode image was used to align the transducer and set the location of the push beam.

2.4.2. Estimation of shear wave speed

The SWE procedure includes generation of a transient shear wave, ultra-fast imaging of propagation of the shear wave and estimation of the local SWS within the tendon. The shear wave was generated by inducing a single focused ultrasound "push" beam with an aperture of 48 elements in the lateral location of the transducer. The lateral push location was chosen to optimise the size of the imaging field of view in the lateral direction (38 mm) and to use the optimum length of the effective elements in the transducer. The focal depth was fixed to 50 wavelengths (15 mm) at mid-depth of the tendon specimen (Fig. 2). The push waveform was transmitted with a 500-cycle pulse at the central frequency of 5 MHz and duration of 100 µs. The push was followed by a 128-element plane wave imaging where the system immediately switched to flash imaging mode and used the same transducer to acquire successive raw radio-frequency data of propagation of the shear wave for 2 ms at a frame rate of 20 kHz. The imaging waveform consisted of one cycle pulse at the central frequency of 5 MHz and produced a set of complex in-phase/quadrature data for each push acquisition. A 2D autocorrelation method [52] was used to calculate tissue displacement fields due to the shear wave along the ultrasonic beam axis and to obtain a spatial-temporal mapping of the axial tissue particle velocity. The SWS was calculated by tracking the time delay in displacement fields at two reference pixels with known distance between them in the lateral direction [53]. The local SWS in the direction of the tendon fibres was then determined as the average of the calculated SWS in the pixels of

the ROI. This estimation is based on the assumption that the ROI is homogenous and SWS is consistent, and also the dispersion effect in the ROI is negligible [43]. The ROI was defined as a 12 by 27 mm rectangle on the surface of the tendon.

2.5. Experimental protocol

The experimental protocol consisted of a patellar tendon tensile test inside a water tank with simultaneous SWE to measure SWS in the tendon at various static loads. The water tank was used to ensure a good coupling between the transducer and tendon specimen for generating the shear wave. The patellar tendon specimen was kept at −18 °C and thawed overnight at room temperature prior to each test. The tendon specimen was then attached to the materials testing machine and the ultrasound transducer was placed in front of the tendon using a clamp (Fig. 1). Prior to each test, the transducer was carefully aligned with the direction of tendon's fibres according to the ultrasound B-mode image of the tendon (Fig. 2) to ensure the SWS is measured in the longitudinal direction of loading. The B-mode image was also used to locate the focal depth of the push and define the ROI. The specimen was then loaded to a pre-defined tensile force, with a crosshead speed of 0.05 mm/s, representing an estimated strain rate of 0.001/s, and then held under static force to perform the SWE measurements (all SWE measurements were performed under static loading of the tendon). This slow strain rate was chosen to minimise the effect of strain rate on the stiffness and mechanical properties of the tendon [54]. At each static load, measures of tendon force and local SWS were acquired. The recorded force was then converted to stress by dividing by the mean CSA of the tendon. The tensile stress was estimated to provide an additional measure for comparing the physiological relevance of loading relative to CSA with the reported stresses in other studies. Eleven loading increments up to 935 N were tested (Table 1). Each trial was repeated six times on one day, and then the whole protocol was repeated on two other days, and the results are presented as a mean of the 18 measurements.

Table 1
Different loads tested during tensile test. σ denotes the normal engineering stress.

Test number	Load (N)	σ (MPa)
1	8	0.06
2	85	0.61
3	175	1.25
4	270	1.93
5	370	2.64
6	460	3.28
7	560	4.00
8	660	4.71
9	755	5.39
10	855	6.10
11	935	6.67

2.6. Statistical analysis

The mean and standard deviation of the local SWS at each load were calculated. A Pearson's product-moment correlation was run to assess the relationship between the tensile force and SWS at each load. A Shapiro-Wilk's test was used to assess whether the variables were normally distributed. As the result of Pearson's correlation test is sensitive to outliers [55], the scatterplot of tensile force and SWS was used to inspect the presence of outliers. All statistical analysis was performed using SPSS software (version 22, Chicago, USA).

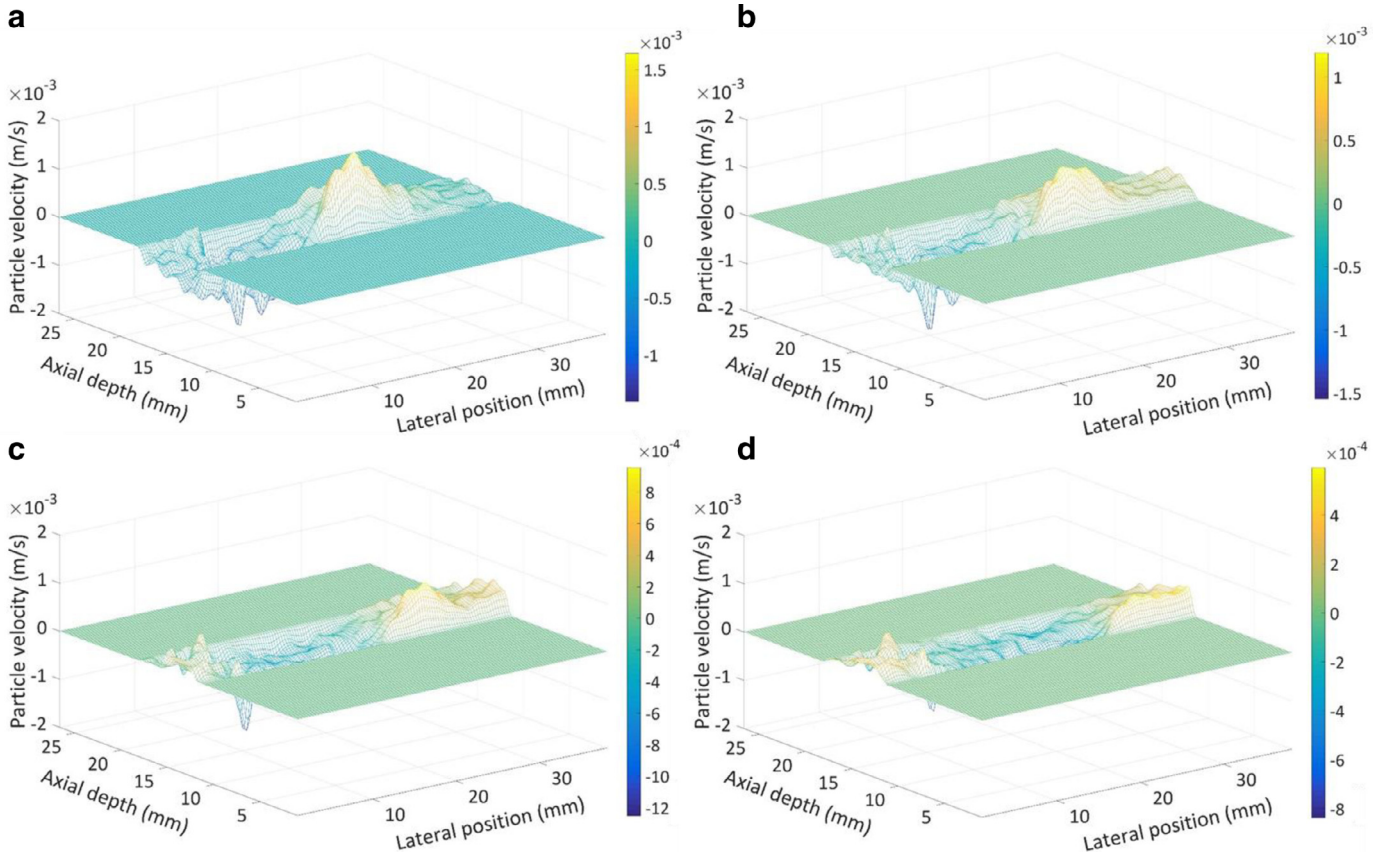

Fig. 3. Axial tissue particle velocity of shear wave propagation at (a) 500 µs (b) 700 µs (c) 900 µs (d) 1100 µs time points, when the patellar tendon specimen is loaded to 460 N. Colorbar shows particle velocity.

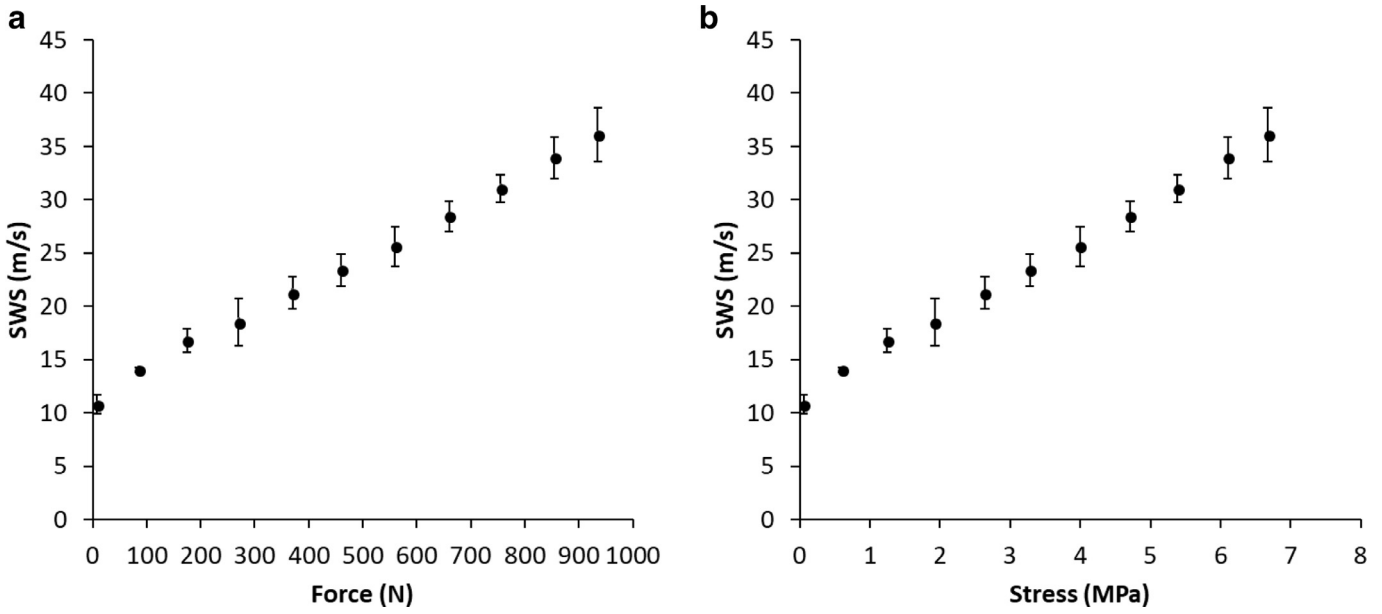

Fig. 4. The relationship between mean local SWS and a) tensile force b) tensile stress for the patellar tendon. Error bars represent the standard deviation ($N = 18$). The error bar is not shown when its size is smaller than the data point.

3. Results

The patellar tendon CSA was measured as 140.1 (± 35.3) mm². The axial tissue particle velocity map of the shear wave propagation was reconstructed for each static load. Fig. 3 shows the propagation of the shear wave in the direction of the tendon's fibres at 460 N at different time points in a typical trial.

The relationship between the mean local SWS, tensile force and tensile stress is shown in Fig. 4. The SWS increased from 10 (± 0.9) m/s to 36 (± 2.6) m/s by increasing the load from 8 N to 935 N.

SWS and load were linearly related, with both variables normally distributed as assessed by Shapiro-Wilk's test ($p > 0.05$), and there were no outliers. The results of Pearson's product-moment correlation test showed a strong positive linear correlation between the mean SWS and load ($r = 0.99$, $p < 0.01$).

4. Discussion and conclusion

The SWE technique and conventional tensile testing were used for the first time to quantify the direct relationship between tensile force, tensile stress and SWS in a human patellar tendon under physiologically-relevant loading. There was a linear correlation between tensile force, tensile stress and SWS. The developed SWE system used in this study measured a maximum SWS of 36.1 m/s for an applied tensile force of 935 N that corresponds to tensile stress of 6.67 MPa. Some other studies have conducted similar studies on animal tendons only at very low loads of up to 10 N, or low stress level of 40 kPa [32,41,56].

The fastest SWS measured using a prevalent commercial SWE system (Aixplorer, SuperSonic Imagine, France) in the literature is 16 m/s [35,36,40,57]. This system has been widely used in many MSK tissue studies [29–31,34–36,38–42]. In addition, Cortes et al. [37] reported a maximum SWS of 20 m/s using another SWE system (Ultrasonix MDP, Ultrasonix, Vancouver, Canada).

Therefore, the results obtained in this study are the largest SWS (36.1 m/s) measured with SWE in the literature. This high SWS allows higher, physiologically-relevant, loads to be measured and so this study also represents the highest tendon loading measured by SWE. The measured tensile force of 935 N is higher than normal patellar tendon loading presented in the literature [58,59]; and is higher than other lower limb tendon loading, such as gastrocnemius [9,60].

There are a number of limitations associated with the study presented in this paper that need to be further improved for clinical application of the SWE technique. Although the range of mechanical loading measured in this study (8-935 N; 0.06-6.67 MPa) can be associated with a range of physiological activities, there are activities that demonstrate much higher tendon loading [50,61] which this system could not measure. Therefore, further improvement in the SWE system is required to measure higher SWS in the MSK tissues during all physiological loading conditions.

The present study is limited to a single cadaveric specimen and the correlation between SWS and load should be further assessed with more specimens to verify reproducibility of the results. The relationship between SWS and load can be then integrated with subject-specific measurements of CSA and strain elastography techniques [13,14] to quantify tendon forces from measured SWS on a subject-specific basis. This provides more accurate estimation of physiological CSA and it can be used to develop regression models for characterising mechanical properties of MSK tissues and quantify the relation between load, stiffness and SWS.

The results from isolated tensile testing in the present study might not be extrapolated directly to interpret in-vivo physiological function of the tendon due to the difference between in-vitro and in-vivo conditions [62]. Therefore, the relationship between SWS and load should be clinically validated by applying the SWE method in-vivo and compare the results with estimation of tendon forces by other means (such as MSK models and force transducers).

In the present study, SWS was determined as the mean SWS within the ROI by assuming a locally homogenous ROI with a uniform strain distribution along the direction of the tendon's fibres. The size and location of ROI was also defined based on the B-mode ultrasound image to minimise the effect of tissue borders on the calculation of SWS. However, tendons may not always exhibit homogenous characteristics at different regions and the size and location of the ROI (particularly at the borders of the tissue) can affect the measurement consistency of SWS [40,63]. Therefore, the influence of size and location of ROI on the calculation of SWS should be further investigated to characterise the sensitivity of SWS to different regions of tendon.

Moreover, SWS was measured in the longitudinal direction of the tendon's fibres by manually aligning the transducer parallel to the loading axis and assuming transversely isotropic characteristics of the tendon [64,65]. This assumption was made as tendons typically exhibit a strong axial symmetry under tensile loading according to the arrangement of collagen fibres [66]. However, it should be noted that the calculation of SWS is highly sensitive to the transducer alignment and the direction of shear wave propagation with respect to the fibre orientation [67,68]. Therefore, the variations of SWS with changes in the transducer alignment should be carefully considered for estimating the anisotropic properties of tendon and comparing the results with in-vivo measurements [28].

In this study, the SWS was measured during static loading of the tendon specimen (constant strain) and the effects of force/stress-relaxation and creep due to tendon viscoelasticity on the SWS was neglected by assuming that the time-variation of stress at each level of loading is small [66]. This assumption is also supported by DeWall et al. [38] who observed no significant temporal changes in SWS within loaded tendons for 30 min. However, synchronous measurement of SWS and tensile force during dynamic tendon loading can eliminate the force/stress-relaxation and creep effects on SWS calculations, and it can provide more information about the characteristics of SWS during dynamic loading conditions, as well as the effect of strain-rate on tendon stiffness. The correlation between SWS and load found in this paper should be further investigated under dynamic loading conditions for in-vivo characterisation of SWS in MSK tissues during different activities (under dynamic loading conditions). This also provides a new opportunity in addition to the conventional methods for characterising mechanical and viscoelastic properties of other soft tissues undergoing cyclic loading, such as human blood vessels [26,43,69] and skin [70,71].

In conclusion, the SWE technique presented in this study has measured the fastest SWS in the literature and has enabled for the first time physiologically-relevant tendon forces to be measured as a function of SWS. This technique can be used as a potential non-invasive direct method to quantify tendon forces for which there are many clinical applications as well as technical applications such as validating MSK models. This approach can be also implemented along with strain elastography techniques to measure localised tissue mechanics in different regions and multiple planes to fully characterise anisotropic, non-linear and viscoelastic properties of tendons as a function of SWS.

Conflict of interest

The authors have no conflict of interest in relation to this work.

Funding

This research did not receive any specific grant from funding agencies in the public, commercial, or not-for-profit sectors.

Ethical approval

Ethical approval was granted from the Tissue Management Committee of the Imperial College Tissue Bank ethics committee (reference number: 12-WA-0196) for using human tissue cadaveric specimen.

References

[1] Cowin SC, Doty SB. Tissue mechanics. Springer Science & Business Media; 2007.
[2] Ooi CC, Malliaras P, Schneider ME, Connell DA. "Soft, hard, or just right?" Applications and limitations of axial-strain sonoelastography and shear-wave elastography in the assessment of tendon injuries. Skelet Radiol 2013;43:1–12.
[3] Dul J, Shiavi R, Green NE. Simulation of tendon transfer surgery. Eng Med 1985;14:31–8.
[4] Delp SL, Loan JP, Hoy MG, Zajac FE, Topp EL, Rosen JM. An interactive graphics-based model of the lower extremity to study orthopaedic surgical procedures. IEEE Trans Biomed Eng 1990;37:757–67.
[5] Erdemir A, McLean S, Herzog W, van den Bogert AJ. Model-based estimation of muscle forces exerted during movements. Clin Biomech 2007;22:131–54.
[6] Pandy MG. Computer modelling and simulation of human movement. Annu Rev Biomed Eng 2001;3:245–73.
[7] Guo J-Y, Zheng Y-P, Xie H-B, Chen X. Continuous monitoring of electromyography (EMG), mechanomyography (MMG), sonomyography (SMG) and torque output during ramp and step isometric contractions. Med Eng Phys 2010;32:1032–42.
[8] Kongsgaard M, Reitelseder S, Pedersen TG, Holm L, Aagaard P, Kjaer M, et al. Region specific patellar tendon hypertrophy in humans following resistance training. Acta Physiol 2007;191:111–21.
[9] Maganaris CN. Tensile properties of in vivo human tendinous tissue. J Biomech 2002;35:1019–27.
[10] O'Brien TD, Reeves ND, Baltzopoulos V, Jones DA, Maganaris CN. Mechanical properties of the patellar tendon in adults and children. J Biomech 2010;43:1190–5.
[11] Pearson SJ, Burgess K, Onambele GNL. Creep and the in vivo assessment of human patellar tendon mechanical properties. Clin Biomech 2007;22:712–17.
[12] Passmore E, Lai A, Sangeux M, Schache AG, Pandy MG. Application of ultrasound imaging to subject-specific modelling of the human musculoskeletal system. Meccanica 2017;52:665–76.
[13] Drakonaki EE, Allen GM, Wilson DJ. Ultrasound elastography for musculoskeletal applications. Br J Radiol 2012;85:1435–45.
[14] Gennisson JL, Deffieux T, Fink M, Tanter M. Ultrasound elastography: principles and techniques. Diagn Interv Imaging 2013;94:487–95.
[15] Bull AJ, Reilly P, Wallace A, Amis A, Emery RH. A novel technique to measure active tendon forces: application to the subscapularis tendon. Knee Surg Sports Traumatol Arthrosc 2005;13:145–50.
[16] Fleming B, Beynnon B. In vivo measurement of ligament/tendon strains and forces: a review. Ann Biomed Eng 2004;32:318–28.
[17] Bercoff J. Ultrafast ultrasound imaging. INTECH; 2011.
[18] Bercoff J, Tanter M, Fink M. Supersonic shear imaging: a new technique for soft tissue elasticity mapping. IEEE Trans Ultrason Ferroelectr Freq Control 2004;51:396–409.
[19] Haen TX, Roux A, Soubeyrand M, Laporte S. Shear waves elastography for assessment of human achilles tendon's biomechanical properties: an experimental study. J Mech Behav Biomed Mater 2017;69:178–84.
[20] Brandenburg JE, Eby SF, Song P, Zhao H, Brault JS, Chen S, et al. Ultrasound elastography: the new frontier in direct measurement of muscle stiffness. Arch Phys Med Rehabil 2014;95:2207–19.
[21] Ferraioli G, Tinelli C, Dal Bello B, Zicchetti M, Filice G, Filice C, et al. Accuracy of real-time shear wave elastography for assessing liver fibrosis in chronic hepatitis C: a pilot study. Hepatology 2012;56:2125–33.
[22] Barr RG, Memo R, Schaub CR. Shear wave ultrasound elastography of the prostate: initial results. Ultrasound Q 2012;28:13–20.
[23] Cosgrove D, Berg W, Doré C, Skyba D, Henry J-P, Gay J, et al. Shear wave elastography for breast masses is highly reproducible. Eur Radiol 2012;22:1023–1032.
[24] Sebag F, Vaillant-Lombard J, Berbis J, Griset V, Henry JF, Petit P, et al. Shear wave elastography: a new ultrasound imaging mode for the differential diagnosis of benign and malignant thyroid nodules. J Clin Endocrinol Metab 2010;95:5281–8.
[25] Mace E, Cohen I, Montaldo G, Miles R, Fink M, Tanter M. In vivo mapping of brain elasticity in small animals using shear wave imaging. IEEE Trans Med Imaging 2011;30:550–8.
[26] Widman E, Maksuti E, Larsson M, Bj A, x00E llmark, et al. Shear wave elastography for characterization of carotid artery plaques - A feasibility study in an experimental setup. In: Proceedings of the IEEE international ultrasonics symposium; 2012. p. 1–4.
[27] Bouillard K, Nordez A, Hug F. Estimation of individual muscle force using elastography. PloS one 2011;6:e29261.
[28] Gennisson J-L, Deffieux T, Macé E, Montaldo G, Fink M, Tanter M. Viscoelastic and anisotropic mechanical properties of in vivo muscle tissue assessed by supersonic shear imaging. Ultrasound Med Biol 2010;36:789–801.
[29] Lacourpaille L, Hug F, Bouillard K, Hogrel JY, Nordez A. Supersonic shear imaging provides a reliable measurement of resting muscle shear elastic modulus. Physiol Meas 2012;33:N19–28.
[30] Leong H-T, Ng GY-f, Leung VY-f, Fu SN. Quantitative estimation of muscle shear elastic modulus of the upper trapezius with supersonic shear imaging during arm positioning. PloS one 2013;8:e67199.
[31] Shinohara M, Sabra K, Gennisson J-L, Fink M, Tanter M. Real-time visualization of muscle stiffness distribution with ultrasound shear wave imaging during muscle contraction. Muscle Nerve 2010;42:438–41.
[32] Eby SF, Song P, Chen S, Chen Q, Greenleaf JF, An K-N. Validation of shear wave elastography in skeletal muscle. J Biomech 2013;46:2381–7.
[33] Wu C-H, Chen W-S, Wang T-G. Elasticity of the coracohumeral ligament in patients with adhesive capsulitis of the shoulder. Radiology 2016;278:458–64.
[34] Aubry S, Nueffer J-P, Tanter M, Becce F, Vidal C, Michel F. Viscoelasticity in achilles tendonopathy: quantitative assessment by using real-time shear-wave elastography. Radiology 2015;274:821–9.
[35] Aubry S, Risson J-R, Kastler A, Barbier-Brion B, Siliman G, Runge M,

et al. Biomechanical properties of the calcaneal tendon in vivo assessed by transient shear wave elastography. Skelet Radiol 2013;42:1143–50.
[36] Chen X-M, Cui L-G, He P, Shen W-W, Qian Y-J, Wang J-R. Shear wave elastographic characterization of normal and torn achilles tendons: a pilot study. J Ultrasound Med 2013;32:449–55.
[37] Cortes DH, Suydam SM, Silbernagel KG, Buchanan TS, Elliott DM. Continuous shear wave elastography: a new method to measure viscoelastic properties of tendons in vivo. Ultrasound Med Biol 2015;41:1518–29.
[38] DeWall RJ, Slane LC, Lee KS, Thelen DG. Spatial variations in Achilles tendon shear wave speed. J Biomech 2014;47:2685–92.
[39] Kot BCW, Zhang ZJ, Lee AWC, Leung VYF, Fu SN. Elastic modulus of muscle and tendon with shear wave ultrasound elastography: variations with different technical settings. PLoS one 2012;7:e44348.
[40] Slane LC, DeWall R, Martin J, Lee K, Thelen DG. Middle-aged adults exhibit altered spatial variations in Achilles tendon wave speed. Physiol Meas 2015;36:1485.
[41] Zhang ZJ, Fu SN. Shear elastic modulus on patellar tendon captured from supersonic shear imaging: correlation with tangent traction modulus computed from material testing system and test retest reliability. PLoS one 2013;8:e68216.
[42] Nordez A, Hug F. Muscle shear elastic modulus measured using supersonic shear imaging is highly related to muscle activity level. J Appl Physiol 2010;108(5):1389–94.
[43] Greenleaf JF, Fatemi M, Insana M. Selected methods for imaging elastic properties of biological tissues. Annu Rev Biomed Eng 2003;5:57–78.
[44] Sarvazyan A, Hall TJ, Urban MW, Fatemi M, Aglyamov SR, Garra BS. An overview of elastography – An emerging branch of medical imaging. Curr Med Imaging Rev 2011;7:255–82.
[45] Tanter M, Bercoff J, Athanasiou A, Deffieux T, Gennisson J-L, Montaldo G, et al. Quantitative assessment of breast lesion viscoelasticity: initial clinical results using supersonic shear imaging. Ultrasound Med Biol 2008;34:1373–86.
[46] Martin JA, Biedrzycki AH, Lee KS, DeWall RJ, Brounts SH, Murphy WL, et al. In vivo measures of shear wave speed as a predictor of tendon elasticity and strength. Ultrasound Med Biol 2015;41:2722–30.
[47] Schechtman H, Bader DL. Fatigue damage of human tendons. J Biomech 2002;35:347–53.
[48] Haut RC, Powlison AC. The effects of test environment and cyclic stretching on the failure properties of human patellar tendons. J Orthop Res 1990;8:532–40.
[49] Cooper DE, Deng XH, Burstein AL, Warren RF. The strength of the central third patellar. tendon graft: a biomechanical study. Am J Sports Med 1993;21:818–24.
[50] Ker RF, Alexander RM, Bennett MB. Why are mammalian tendons so thick? J Zool 1988;216:309–24.
[51] Goodship AE, Birch HL. Cross sectional area measurement of tendon and ligament in vitro: a simple, rapid, non-destructive technique. J Biomech 2005;38:605–8.
[52] Loupas T, Powers JT, Gill RW. An axial velocity estimator for ultrasound blood flow imaging, based on a full evaluation of the Doppler equation by means of a two-dimensional autocorrelation approach. IEEE Trans Ultrason Ferroelectr Freq Control 1995;42:672–88.
[53] Nordenfur T. Comparison of pushing sequences for shear wave elastography. KTH School of Technology and Health; 2013.
[54] Bonner TJ, Newell N, Karunaratne A, Pullen AD, Amis AA, Bull A MJ, et al. Strain-rate sensitivity of the lateral collateral ligament of the knee. J Mech Behav Biomed Mater 2015;41:261–70.
[55] Wilcox R. Inferences Based on a Skipped Correlation Coefficient. J Appl Stat 2004;31:131–43.
[56] Yeh C-L, Kuo P-L, Li P-C. Correlation between the shear wave speed in tendon and its elasticity properties. IEEE Int Ultrason Symp 2013:9–12.
[57] Brum J, Bernal M, Gennisson JL, Tanter M. In vivo evaluation of the elastic anisotropy of the human Achilles tendon using shear wave dispersion analysis. Phys Med Biol 2014;59:505.
[58] Ahmed A, Burke D, Hyder A. Force analysis of the patellar mechanism. J Orthop Res 1987;5:69–85.
[59] Shelburne KB, Torry MR, Pandy MG. Muscle, ligament, and joint-contact forces at the knee during walking. Med Sci Sports Exerc 2005;37:1948–56.
[60] Finni T, Komi PV, Lukkariniemi J. Achilles tendon loading during walking: application of a novel optic fiber technique. Eur J Appl Physiol 1998;77:289–291.
[61] Cleather DJ, Goodwin JE, Bull AMJ. Hip and knee joint loading during vertical jumping and push jerking. Clin Biomech (Bristol, Avon) 2013;28:98–103.
[62] Maganaris CN, Paul JP. Tensile properties of the in vivo human gastrocnemius tendon. J Biomech 2002;35:1639–46.
[63] Magnusson SP, Hansen P, Aagaard P, Brond J, Dyhre-Poulsen P, Bojsen-Moller J, et al. Differential strain patterns of the human gastrocnemius aponeurosis and free tendon, in vivo. Acta Physiol Scand 2003;177:185–95.
[64] Fang F, Lake SP. Modelling approaches for evaluating multiscale tendon mechanics. Interface Focus 2016;6:20150044.
[65] Royer D, Gennisson J-L, Deffieux T, Tanter M. On the elasticity of transverse isotropic soft tissues (L). J Acoust Soc Am 2011;129:2757–60.
[66] Kuo P-L, Li P-C, Li M-L. Elastic properties of tendon measured by two different approaches. Ultrasound Med Biol 2001;27:1275–84.
[67] Chatelin S, Bernal M, Papadacci C, Gennisson JL, Tanter M, Pernot M. Anisotropic polyvinyl alcohol hydrogel phantom for shear wave elastography in fibrous biological soft tissue. In: Proceedings of the IEEE international ultrasonics symposium; 2014. p. 1857–60.
[68] Wang M, Byram B, Palmeri M, Rouze N, Nightingale K. Imaging transverse isotropic properties of muscle by monitoring acoustic radiation force induced shear waves using a 2-D matrix ultrasound array. IEEE Trans Med Imaging 2013;32:1671–84.
[69] Schmitt C, Soulez G, Maurice RL, Giroux M-F, Cloutier G. Noninvasive vascular elastography: toward a complementary characterization tool of atherosclerosis in carotid arteries. Ultrasound Med Biol 2007;33:1841–1858.
[70] Pailler-Mattei C, Bec S, Zahouani H. In vivo measurements of the elastic mechanical properties of human skin by indentation tests. Med Eng Phys 2008;30:599–606.
[71] Manschot JFM, Brakkee AJM. The measurement and modelling of the mechanical properties of human skin in vivo—I. The measurement. J Biomech. 1986;19:511–15.